

See discussions, stats, and author profiles for this publication at: <https://www.researchgate.net/publication/6619604>

# Vaporization Thermodynamic Studies by High-Temperature Mass Spectrometry on Some Three-Phase Regions over the MnO–TeO<sub>2</sub> Binary Line in the Mn–Te–O Ternary System

ARTICLE in THE JOURNAL OF PHYSICAL CHEMISTRY A · JANUARY 2007

Impact Factor: 2.69 · DOI: 10.1021/jp064011b · Source: PubMed

---

CITATIONS

5

---

READS

13

3 AUTHORS, INCLUDING:



Sai Baba Magapu

Indira Gandhi Centre for Atomic Research

49 PUBLICATIONS 459 CITATIONS

SEE PROFILE

# Univariant Three- and Four-Phase Vaporization Equilibria in the Ternary Mn–Te–O System: A High-Temperature Mass Spectrometric Study of Binary $x\text{MnO} + (1 - x)\text{TeO}_2$ with $x \geq 0.5$

T. S. Lakshmi Narasimhan, M. Sai Baba, and R. Viswanathan\*

Materials Chemistry Division, Indira Gandhi Centre for Atomic Research, Kalpakkam, Tamil Nadu 603 102, India

Received: December 31, 2001; In Final Form: April 23, 2002

High-temperature mass spectrometric studies on  $x\text{MnO} + (1 - x)\text{TeO}_2$  samples with  $x = 0.50, 0.54, 0.57, 0.67, 0.75$ , and  $0.79$  were conducted to investigate the vaporization behavior of the MnO–TeO<sub>2</sub> binary system. Along with MnTeO<sub>3</sub>, a phase of equimolar composition, another ternary phase Mn<sub>3</sub>TeO<sub>6</sub> lying on the oxygen-rich side of the MnO–TeO<sub>2</sub> binary line was generated during preparations as well as during isothermal dynamic effusion experiments. Experiments were also conducted by adding a known excess of MnO or Mn to aliquots from different samples to examine whether the resulting condensed phase–vapor phase equilibrium would preclude or at least retard the buildup of Mn<sub>3</sub>TeO<sub>6</sub>. On the contrary, these experiments, many being characterized by high Te<sub>2</sub>(g) evolution in the initial stages, yielded residues of MnTeO<sub>3</sub> + Mn<sub>3</sub>TeO<sub>6</sub> or Mn<sub>3</sub>O<sub>4</sub> + Mn<sub>3</sub>TeO<sub>6</sub>, the latter when the MnO addition was such that the resulting overall  $x(\text{MnO})$  was as high as 0.80. The vapor phase in all cases consisted only of Te- and O-bearing species: TeO<sub>2</sub>, TeO, Te<sub>2</sub>, and O<sub>2</sub>. These observations led to the inference that the MnO-rich region of the MnO + TeO<sub>2</sub> system is not inclined to remain binary during vaporization. Anomalous vaporization behavior was observed for Te<sub>2</sub>(g) in some isothermal experiments. While for all other gaseous species monotonic decrease in partial pressures ended with values stabilizing around the respective minimum, that in the  $p(\text{Te}_2)$  ended with a turn-around in its value; there was a rapid increase to eventually stabilize at a value that was not only about four times higher than the minimum but also even higher than that measured before the onset of monotonic decrease. These features and other aspects associated with different univariant vaporization equilibria in the Mn–Te–O ternary system are discussed.

## Introduction

Tellurium is one of the very volatile and reactive fission products generated during nuclear fission. It is believed to play an important role in fuel-clad chemical interactions in mixed-oxide-fueled fast reactors.<sup>1</sup> Vaporization thermodynamic studies on tellurium and its compounds with oxygen or clad components or both, therefore, are of great importance in better understanding of clad corrosion and source-term parameters. Having conducted studies on tellurium,<sup>2</sup> tellurium dioxide,<sup>3</sup> and binary systems of tellurium with stainless steel clad components,<sup>4–13</sup> we are focusing our attention on the ternary M–Te–O systems, and particularly on the binary sections involving MO<sub>x</sub> and TeO<sub>2</sub>. To begin with, a detailed study of phase equilibria in the Mn–Te–O system was undertaken.

The ternary compounds known<sup>14–18</sup> in the Mn–Te–O system are as follows: Mn<sub>6</sub>Te<sub>5</sub>O<sub>16</sub>, MnTeO<sub>3</sub>, Mn<sub>2</sub>Te<sub>3</sub>O<sub>8</sub>, MnTe<sub>2</sub>O<sub>5</sub>, and MnTe<sub>6</sub>O<sub>13</sub> (phases along the MnO–TeO<sub>2</sub> binary line); Mn<sub>3</sub>TeO<sub>6</sub> (a 3:1 phase along the MnO–TeO<sub>3</sub> line or a 1:1 phase along the Mn<sub>3</sub>O<sub>4</sub>–TeO<sub>2</sub> line); Mn<sub>2</sub>TeO<sub>6</sub> (a 2:1 phase along the MnO<sub>2</sub>–TeO<sub>2</sub> binary line). While the phase diagram<sup>17</sup> for the MnO–TeO<sub>2</sub> binary system with  $x(\text{MnO}) = 0–0.5$  and heat capacities<sup>18</sup> for MnTeO<sub>3</sub>, Mn<sub>2</sub>Te<sub>3</sub>O<sub>8</sub>, and MnTe<sub>2</sub>O<sub>5</sub> are reported in the literature, no vaporization study exist nor does a composition diagram depicting the existence of different three-

phase regions. There is also some doubt as to whether Mn<sub>6</sub>Te<sub>5</sub>O<sub>16</sub> (formerly designated as Mn<sub>4</sub>Te<sub>3</sub>O<sub>10</sub>) is really a stable phase<sup>14</sup> and thus qualified to be the most MnO-rich phase in the MnO–TeO<sub>2</sub> binary system in view of its tendency to decompose to MnTeO<sub>3</sub> and Mn<sub>3</sub>TeO<sub>6</sub> on being heated for long duration at  $T = 923$  K. Our investigations in the Mn–Te–O system had the objectives of filling these gaps.

In this paper, we report results of our attempts to prepare samples along the MnO–TeO<sub>2</sub> binary line (with  $x(\text{MnO}) \geq 0.5$ ) and of vaporization studies on different aliquots from these samples. This composition region was chosen primarily with the aim of identifying the most MnO-rich phase of the MnO–TeO<sub>2</sub> system by (1) direct preparation from MnO and TeO<sub>2</sub> powders, with successively increasing  $x(\text{MnO})$  such that one eventually obtains the biphasic sample of MnO + Mn<sub>x</sub>Te<sub>y</sub>O<sub>x+2y</sub> and (2) continuous vaporization under effusion conditions of aliquots of samples with different initial  $x(\text{MnO})$ . If the vaporization were to involve preferential loss of the TeO<sub>2</sub> component, as in the case of NiO–TeO<sub>2</sub> system,<sup>19</sup> then at some time, one would obtain as vaporization residue a two-phase mixture of MnO + Mn<sub>x</sub>Te<sub>y</sub>O<sub>x+2y</sub> with  $x \geq y$ . Interestingly, however, our preparations, as well as effusion experiments, never yielded MnO as the coexisting phase; instead, they always gave Mn<sub>3</sub>TeO<sub>6</sub> as one of the phases and, in effusion experiments, its buildup in the residue. Because this phase does not lie on the MnO–TeO<sub>2</sub> binary line and is on the O-rich side of it, its formation must be caused by some source of oxygen supply,

\* To whom correspondence should be addressed. Fax: 91 4114 480065. E-mail: rvis@igcar.ernet.in.

as evidenced by its preparation in pure form when a mixture of MnO and TeO<sub>2</sub> in the molar ratio of 3:1 was heated in air. Many of our effusion experiments showed indications of univariant three-phase equilibria involving Mn<sub>3</sub>TeO<sub>6</sub> + MnTeO<sub>3</sub> + vapor and Mn<sub>3</sub>TeO<sub>6</sub> + Mn<sub>3</sub>O<sub>4</sub> + vapor. In some of the effusion experiments with samples having three condensed phases, Mn<sub>3</sub>TeO<sub>6</sub>, MnTeO<sub>3</sub>, and Mn<sub>2</sub>Te<sub>3</sub>O<sub>8</sub>, the system reached the former equilibrium after exhibiting a rather anomalous vaporization behavior with respect to Te<sub>2</sub>(g). The chemistry concerning such vaporization equilibria is discussed in this paper.

## Experimental Section

Samples were prepared by direct reaction at  $T = 950$  or  $975$  K of MnO (Aldrich Chemical Co., Inc., purity 99.99%) and TeO<sub>2</sub> (Leico Industries, Inc., purity 99.99%) powders in sealed containers or of MnCO<sub>3</sub> (Aldrich Chemical Co., Inc., purity 99.9%) and TeO<sub>2</sub> under dynamic argon flow. Thoroughly ground and homogenized mixtures were made into pellets of 10 mm diameter and heated in a platinum crucible or boat. Totally, 11 samples were prepared by employing four methods, two static, one dynamic, and one in open air.

With use of method 1, three samples with initial  $x(\text{MnO}) = 0.50$  (sample 1),  $0.57$  (sample 2), and  $0.67$  (sample 3) were prepared. A platinum crucible containing the pellets was placed inside a long stainless steel cylindrical vessel (length = 320 mm and diameter = 45 mm) having a knife-edged flange at the top to permit sealing with a blank flange and a copper gasket. The vessel was alternately evacuated and flushed with argon several times before being isolated with argon present inside at a pressure of  $\geq 10^5$  Pa. Heating was done in two or three cycles. At the end of each cycle, the pellets were taken out after being cooled to room temperature, ground, and either repelletized if they were to be heated again or stored in vials inside an argon-atmosphere glovebox to be used later for vaporization experiments. The pellets were heated for 15–20 h at 875 K in the first cycle and for an equal duration at 975 K (sample 1) or 950 K (samples 2 and 3) in the final cycle. In the case of sample 2, an intermediate cycle with  $T = 925$  K for 15 h was employed.

With the use of method 2, four samples with initial  $x(\text{MnO}) = 0.50$  (sample 4),  $0.54$  (sample 5), and  $0.79$  (samples 6 and 7) were prepared. The pellets were enveloped with a platinum foil (or placed in a platinum boat) and inserted into a quartz tube (length = 80–100 mm and diameter = 15 mm), which was alternately evacuated and flushed with argon several times before being sealed under a residual pressure of  $\sim 10^{-4}$  Pa. The pellets were heated at 875 K for 24 h and at 950 K for 60 h.

With the use of method 3, two samples with initial  $x(\text{MnCO}_3) = 0.50$  (sample 8) and  $0.79$  (sample 9) were heated in a dynamic mode under flowing argon. The pellets were placed in a platinum boat and inserted into a long horizontal quartz tube (length = 70 cm and diameter = 35 mm), the inlet of which was connected to the argon gas cylinder through a dehydrating medium and the outlet into water kept inside a beaker. The pellets were heated at 875 K for 8–10 h and at 950 K for 15–20 h.

With the use of method 4, two samples with initial  $x(\text{MnO}) = 0.75$  (samples 10 and 11) were prepared by heating at 950 K for about 24 h in air. The platinum boat containing the pellets was kept at the uniform temperature zone of a horizontal furnace.

The samples prepared by using methods 2, 3, and 4 were ground and stored in vials, kept in a vacuum desiccator. Table 1 gives the details of the samples prepared and results of X-ray diffraction analysis.

**TABLE 1: Details of Different Samples  $x\text{MnO} + (1 - x)\text{TeO}_2$  Prepared and the Condensed Phases Identified**

sample no.	starting $x(\text{MnO})$	condensed phases identified in the sample	
		on the MnO–TeO <sub>2</sub> binary line	outside the MnO–TeO <sub>2</sub> binary line
Method 1: Static (Argon Atmosphere)			
1	0.50 <sup>a</sup>	MnTeO <sub>3</sub>	Mn <sub>3</sub> TeO <sub>6</sub>
2	0.57	MnTeO <sub>3</sub> , Mn <sub>2</sub> Te <sub>3</sub> O <sub>8</sub>	Mn <sub>3</sub> TeO <sub>6</sub>
3	0.67	MnTeO <sub>3</sub> , Mn <sub>2</sub> Te <sub>3</sub> O <sub>8</sub>	Mn <sub>3</sub> TeO <sub>6</sub>
Method 2: Static (Residual Pressure of $1 \times 10^{-4}$ Pa)			
4	0.50	MnTeO <sub>3</sub> , Mn <sub>2</sub> Te <sub>3</sub> O <sub>8</sub>	Mn <sub>3</sub> TeO <sub>6</sub>
5	0.54	MnTeO <sub>3</sub> , Mn <sub>2</sub> Te <sub>3</sub> O <sub>8</sub>	Mn <sub>3</sub> TeO <sub>6</sub>
6	0.79	MnTeO <sub>3</sub>	Mn <sub>3</sub> TeO <sub>6</sub> , Mn <sub>3</sub> O <sub>4</sub>
7	0.79 <sup>b</sup>	MnTeO <sub>3</sub> , Mn <sub>6</sub> Te <sub>5</sub> O <sub>16</sub>	Mn <sub>3</sub> O <sub>4</sub>
Method 3: Dynamic (Flowing Argon)			
8	0.50 <sup>c</sup>	MnTeO <sub>3</sub> , Mn <sub>2</sub> Te <sub>3</sub> O <sub>8</sub>	Mn <sub>3</sub> TeO <sub>6</sub>
9	0.79 <sup>c</sup>	MnTeO <sub>3</sub>	Mn <sub>3</sub> TeO <sub>6</sub> , Mn <sub>3</sub> O <sub>4</sub>
Method 4: In Open-Air			
10	0.75		Mn <sub>3</sub> TeO <sub>6</sub>
11	0.75		Mn <sub>3</sub> TeO <sub>6</sub>

<sup>a</sup> Final preparation temperature was 975 K, while for all other samples, it was 950 K. <sup>b</sup> MnO used was that obtained by heating MnCO<sub>3</sub> at 925 K under flowing hydrogen atmosphere. <sup>c</sup>  $x(\text{MnCO}_3)$ .

The vaporization experiments were conducted with a VG micromass MM 30 BK Knudsen-cell mass spectrometer. The instrument has been described previously.<sup>2–13</sup> Two series of vaporization experiments were conducted: series 1 using aliquots directly taken from bulk-samples and series 2 after adding calculated amounts of MnO (series 2a) or Mn (series 2b) to aliquots from bulk samples and mixing them to make the overall composition to desired values. One experiment (series 2c) was conducted by adding Mn<sub>3</sub>O<sub>4</sub> to the vaporization residue of a series 1 experiment. A platinum crucible, placed inside an alumina Knudsen cell, was used to contain the samples. The experiments reported in this paper are mainly isothermal ( $T = 950$  K) and consisted of measurement of ion intensities as a function of time at an electron-impact energy of 37 eV. This rendered it possible to examine how the ion intensities (or the vaporization behavior) varied with time. Ion-focusing conditions were optimized to get highest intensity for the ion TeO<sub>2</sub><sup>+</sup>. In many experiments, ion intensities were also measured at least once at 13 eV at which fragmentation is minimized. All vaporization residues were subjected to X-ray diffraction analysis. Table 2 gives the details of different series of experiments and is grouped according to the phases identified in the vaporization residues. Periodic investigations were conducted on TeO<sub>2</sub>(s) to compare its known congruent effusion behavior with that observed in the case of experiments in the Mn–Te–O system.

## Results

The ions detected in the mass spectra of vapor over different Mn–Te–O samples were Te<sup>+</sup>, Te<sub>2</sub><sup>+</sup>, TeO<sup>+</sup>, TeO<sub>2</sub><sup>+</sup>, and O<sub>2</sub><sup>+</sup>. Accordingly, only Te- and O-bearing gaseous species constitute the vapor phase: Te<sub>2</sub>, TeO, TeO<sub>2</sub>, and O<sub>2</sub>. The ion Te<sup>+</sup> arose due to dissociative ionization, mainly of TeO(g). Because of high background for the ion O<sub>2</sub><sup>+</sup>, its net intensity (difference between the values corresponding to “shutter-open” and “shutter-close” conditions) was not meaningful except at high values.

Because freshly loaded samples were slowly heated to 950 K, the series 2a and 2b experiments (except experiment 27) were characterized by significant evolution of Te<sub>2</sub>(g) at  $T > 800$  K, about 2 orders of magnitude higher than in other series.

**TABLE 2: Details of Samples Employed in Isothermal Vaporization Experiments at  $T = 950$  K and of the Corresponding Residues**

sample no.	expt no.	initial overall composition $\text{Mn}_x\text{Te}_y\text{O}_z$			duration (min)	phases present in the starting sample	remarks on the residue
		$x$	$y$	$z$			
Residue $\text{MnTeO}_3 + \text{Mn}_3\text{TeO}_6$							
series 1: direct aliquots from bulk samples							
1	7	0.200	0.200	0.600	330	$\text{MnTeO}_3 + \text{Mn}_3\text{TeO}_6$	build up of $\text{Mn}_3\text{TeO}_6$
	8				680		
	9				1899		
	20				2049		
2	32	0.235	0.177	0.588	384	$\text{Mn}_2\text{Te}_3\text{O}_8 + \text{MnTeO}_3 + \text{Mn}_3\text{TeO}_6$	$\text{Mn}_2\text{Te}_3\text{O}_8$ disappeared;
3	13	0.286	0.143	0.571	453		build up of $\text{Mn}_3\text{TeO}_6$ .
4	16	0.200	0.200	0.600	2043		
	18				3281		
5	21	0.217	0.189	0.594	2041		
	30				1987		
Residue $\text{MnTeO}_3 + \text{Mn}_3\text{TeO}_6 + \text{Mn}_3\text{O}_4$							
series 1: direct aliquots from bulk samples							
6	22	0.356	0.096	0.548	484	$\text{MnTeO}_3 + \text{Mn}_3\text{TeO}_6 + \text{Mn}_3\text{O}_4$	all three phases retained
	26				206		
9	46	0.356	0.096	0.548	278		
series 2c: $\text{Mn}_3\text{O}_4$ mixed with residues of 16 and 18							
	28	$a$	$a$	$a$	400	$\text{Mn}_3\text{O}_4 + (\text{MnTeO}_3 + \text{Mn}_3\text{TeO}_6)$	all three phases retained
Residue $\text{Mn}_3\text{TeO}_6 + \text{Mn}_3\text{O}_4$							
series 1: direct aliquots from bulk samples							
6	23	0.356	0.096	0.548	752	$\text{Mn}_3\text{TeO}_6 + \text{MnTeO}_3 + \text{Mn}_3\text{O}_4$	$\text{MnTeO}_3$ disappeared
10	34	0.300	0.100	0.600	484	$\text{Mn}_3\text{TeO}_6$	$\text{Mn}_3\text{O}_4$ generated
series 2a: $\text{MnO}$ mixed with aliquots from bulk samples							
1	10	0.357	0.095	0.548	521	$\text{MnO} + (\text{MnTeO}_3 + \text{Mn}_3\text{TeO}_6)$	added $\text{MnO}$ disappeared;
	11	0.365	0.090	0.545	1642		so did $\text{MnTeO}_3$ ; $\text{Mn}_3\text{O}_4$ generated;
2	15	0.364	0.090	0.545	697	$\text{MnO} + (\text{MnTeO}_3 + \text{Mn}_3\text{TeO}_6 + \text{Mn}_2\text{Te}_3\text{O}_8)$	in addition $\text{Mn}_2\text{Te}_3\text{O}_8$ also disappeared
3	12	0.364	0.091	0.545	411		
	14				779		
series 2b: $\text{Mn}$ mixed with aliquots from bulk samples							
2	31	0.310	0.16	0.530	327	$\text{Mn} + (\text{MnTeO}_3 + \text{Mn}_3\text{TeO}_6 + \text{Mn}_2\text{Te}_3\text{O}_8)$	added $\text{Mn}$ disappeared;
	35	0.378	0.124	0.498	436		so did $\text{MnTeO}_3$ and $\text{Mn}_2\text{Te}_3\text{O}_8$ ; $\text{Mn}_3\text{O}_4$ generated
10	36	0.381	0.088	0.531	575	$\text{Mn} + (\text{Mn}_3\text{TeO}_6)$	added $\text{Mn}$ disappeared; $\text{Mn}_3\text{O}_4$ generated.
Residue $\text{MnO} + \text{Mn}_3\text{O}_4$							
series 2a: $\text{MnO}$ mixed with aliquots from bulk samples							
6	24	0.427	0.049	0.524	417	$\text{MnO} + (\text{Mn}_3\text{TeO}_6 + \text{MnTeO}_3 + \text{Mn}_3\text{O}_4)$	added $\text{MnO}$ present, both $\text{MnTeO}_3$ and $\text{Mn}_3\text{TeO}_6$ disappeared
	25				387		
Residue $\text{Mn} + \text{MnO} + \text{MnTe}$							
series 2b: $\text{Mn}$ mixed with aliquots from bulk samples							
3	27	0.60	0.08	0.32	529	$\text{Mn} + (\text{Mn}_3\text{TeO}_6 + \text{MnTeO}_3 + \text{Mn}_2\text{Te}_3\text{O}_8)$	all ternary phases disappeared
Residue $\text{MnTeO}_3 + \text{Mn}_6\text{Te}_5\text{O}_{16} + \text{Mn}_3\text{O}_4$							
series 1: direct aliquots from bulk samples							
7	43	0.356	0.096	0.548	739	$\text{MnTeO}_3 + \text{Mn}_6\text{Te}_5\text{O}_{16} + \text{Mn}_3\text{O}_4$	all three phases retained

<sup>a</sup> Unknown composition.

In the case of experiment 27, no significant signal for any ion was obtained even after  $\sim 9$  h of heating at 950 K, an observation consistent with the vaporization behavior expected for the resulting residue, a three-phase mixture of  $\text{Mn} + \text{MnO} + \text{MnTe}$ .

Figures 1–4 show results obtained in those experiments in which we observed consistent turn arounds in the ion intensity of  $\text{Te}_2^+$ . The  $I(\text{Te}_2^+)$ , which was monotonically decreasing, reached a minimum after which it steeply increased to reach an invariant value, which is at least 3 times higher than the minimum value.

A section of the phase diagram for the  $\text{Mn}-\text{Te}-\text{O}$  system, with  $\text{MnO}$ ,  $\text{TeO}_2$ , and  $\text{Mn}_3\text{O}_4$  as the terminal phases, is depicted in Figure 5. The four-phase vaporization equilibria are labeled with plain numbers, while the three-phase vaporization equilibria are labeled with circled numbers.

## Discussion

**Sample Preparation.** Table 1 shows that none of our preparations yielded  $\text{MnO}$  as one of the phases, even those with high  $x(\text{MnO})$ , nor did they yield only the phases that lie along the  $\text{MnO}-\text{TeO}_2$  binary line, although all preparations effectively had only these two constituents. On the contrary, either  $\text{Mn}_3\text{TeO}_6$  or  $\text{Mn}_3\text{O}_4$ , the phases that are on the O-rich side of the binary line, was also formed in samples 1–9. Samples 10 and 11, preparations of which were carried out with  $x(\text{MnO}) = 0.75$  and in open-air, contained the single-phase  $\text{Mn}_3\text{TeO}_6$ . Similar preparation with  $x(\text{MnO}) = 1$  in open air yielded a single-phase  $\text{Mn}_3\text{O}_4$ . One makes a quick inference from these observations: an oxygen supply was present from somewhere in preparation of samples 1–9, regardless of care taken to minimize it in

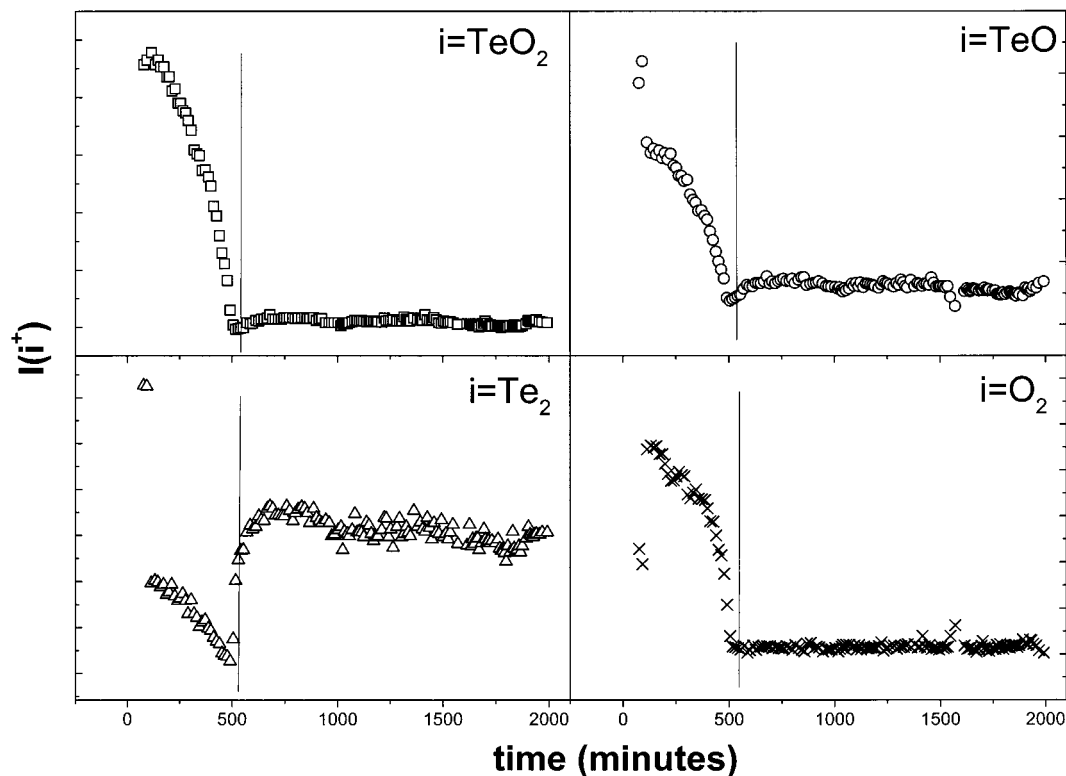


**Figure 1.** Variation of ion intensities with time in experiment 16 (sample 4 of starting composition  $0.50\text{MnO} + 0.50\text{TeO}_2$  and phases  $\text{Mn}_2\text{Te}_3\text{O}_8 + \text{MnTeO}_3 + \text{Mn}_3\text{TeO}_6$ ; initial mass = 0.064 73 g). The line of demarcation, drawn at  $t = 530$  min, serves to indicate that the system became univariant after a turn around in  $I(\text{Te}_2^+)$ , and with only two condensed phases ( $\text{MnTeO}_3 + \text{Mn}_3\text{TeO}_6$ ) in equilibrium with the vapor phase. The final composition, as estimated from the total mass loss of 0.009 59 g, is  $\text{O}/(\text{Mn} + \text{Te}) = 1.5$  and  $\text{O}/\text{Te} = 3.4$ .

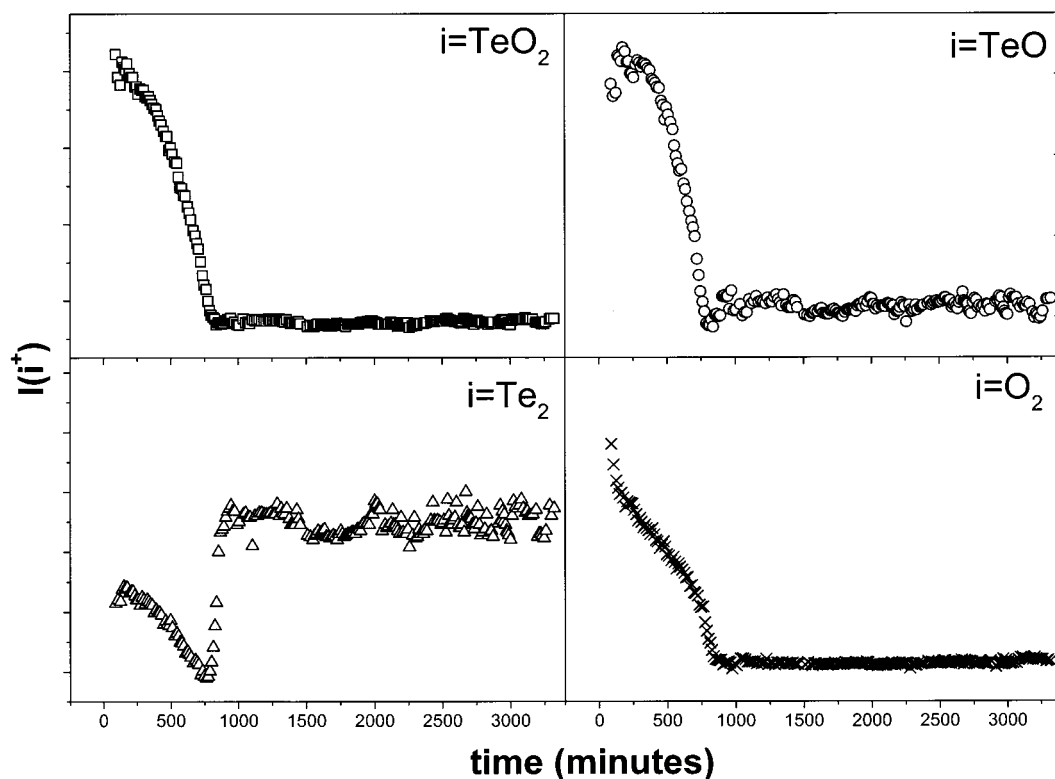


**Figure 2.** Ion intensities variation with time in experiment 18 (another aliquot of sample 4; initial mass = 0.065 56 g), providing confirmation of features shown in Figure 1. The final composition, as estimated from the total mass loss of 0.011 66 g, is  $\text{O}/(\text{Mn} + \text{Te}) = 1.5$  and  $\text{O}/\text{Te} = 3.5$ .

different methods of preparation. Either or both of the following factors might have contributed to formation of phases other than those on the binary line: (1) the manganese monoxide used in preparations was hyperstoichiometric; (2) the vapor phase was

composed of species of which the overall Te/O ratio was greater than 1:2. The extent to which each of these factors might have dictated the results of different methods of preparations is difficult to estimate. The effect of vaporization behavior

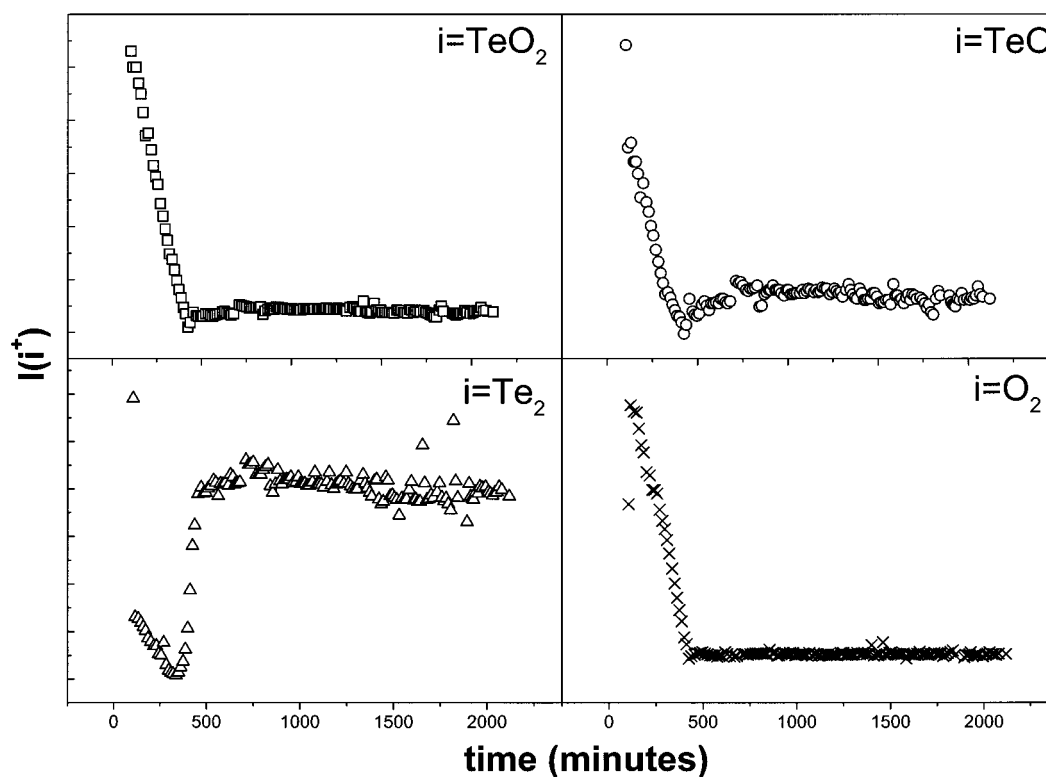


**Figure 3.** Variation of ion intensities with time in experiment 21 (sample 5 of starting composition  $0.54\text{MnO} + 0.46\text{TeO}_2$  and phases  $\text{Mn}_2\text{Te}_3\text{O}_8 + \text{MnTeO}_3 + \text{Mn}_3\text{TeO}_6$ ; initial mass = 0.065 52). The sample shows a continuous decrease in ion intensities from the start of the experiment, but subsequent features are similar to those shown in Figures 1 and 2. The final composition, as estimated from the total mass loss of 0.006 11 g, is  $\text{O}/(\text{Mn} + \text{Te}) = 1.5$  and  $\text{O}/\text{Te} = 3.5$ .

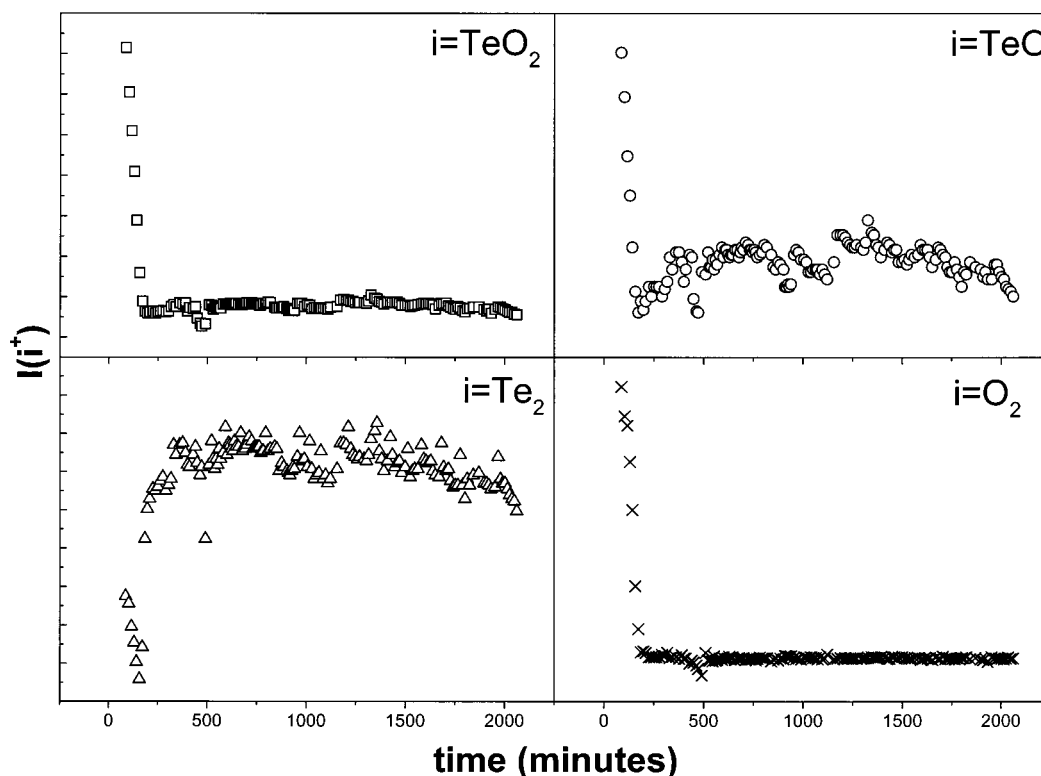


**Figure 4.** Ion intensities variation with time in experiment 30 (another aliquot of sample 5; initial mass = 0.031 93), providing confirmation of features shown in Figure 3. The final composition, as estimated from the total mass loss of 0.009 50 g, is  $\text{O}/(\text{Mn} + \text{Te}) = 1.5$  and  $\text{O}/\text{Te} = 4.8$ .

(associated with different reactions) would be higher in the dynamic mode of preparation (method 3) and, even in static mode, in case some portion of the preparation setup acted as a

vapor sink (method 1). Other aspects pertinent to generation of  $\text{Mn}_3\text{TeO}_6$  along with  $\text{MnTeO}_3$  or  $\text{Mn}_3\text{O}_4$  or both are discussed later.



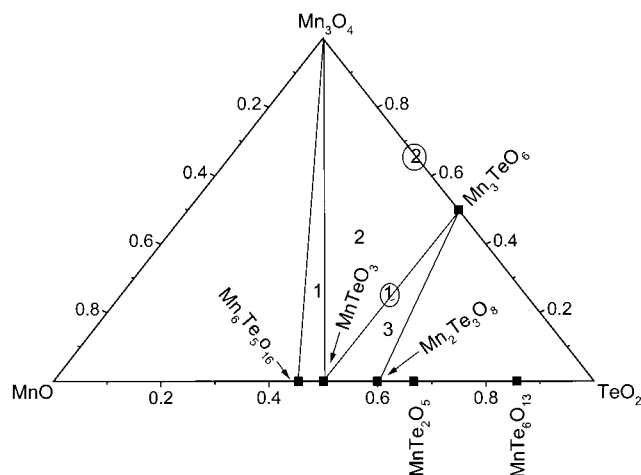


**Figure 5.** A section of the phase diagram for the Mn–Te–O system at  $T = 950$  K. The plain numbers represent the four-phase equilibria, and the circled numbers represent the three-phase equilibria discussed in the text.

**Residues from Effusion Experiments.** Table 2 shows that our different effusion experiments yielded residues of varying nature, evidently determined by vaporization behaviors (appropriate for the equilibria that existed at different stages) and duration of the experiments. Only in three experiments (24 and 25 of series 2a, and 27 of series 2b) did we obtain residues containing the MnO phase but, ironically, no ternary phase.

**Residue  $\text{MnTeO}_3 + \text{Mn}_3\text{TeO}_6$ .** The series 1 experiments, conducted with samples 1–5, all yielded as residue a two-phase mixture of  $\text{MnTeO}_3 + \text{Mn}_3\text{TeO}_6$ . If the continuous vaporization experiments with sample 1 (experiments 7, 8, 9, and 20) involved the retention of these two phases, those with samples 2–5 (experiments 13, 16, 18, 21, 30, and 32) involved the disappearance of  $\text{Mn}_2\text{Te}_3\text{O}_8$ . The experiment 20 revealed retention of the two phases even after continuous vaporization for  $\sim 2050$  min, the ion intensities remaining invariant with time throughout. In experiment 32 (as well as in experiment 13), it looked as though the disappearance of  $\text{Mn}_2\text{Te}_3\text{O}_8$  occurred before the system reached  $T = 950$  K, because the ion intensities did not vary much from the beginning. In experiments 16 and 18 (sample 4) and 21 and 30 (sample 5), however, the disappearance of  $\text{Mn}_2\text{Te}_3\text{O}_8$  produced striking changes in ion intensities, especially with respect to  $\text{Te}_2^+$ , before giving rise to long hours of stability (see Figures 1–4). All of these observations led to the following inference: an invariant three-phase vaporization equilibrium (which we will denote as 3PEQ1) occurs when the two solids  $\text{MnTeO}_3$  and  $\text{Mn}_3\text{TeO}_6$  are present, with the latter not lying on the MnO– $\text{TeO}_2$  binary line, and progressively getting built up. The existence of such an interesting vaporization equilibrium, hitherto unreported (to our knowledge) in ternary M–Te–O systems, needs to be supported by a valid thermodynamic reasoning, which we do later.

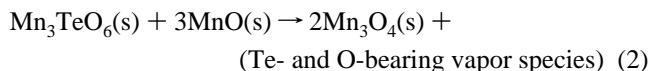
**Residue  $\text{MnTeO}_3 + \text{Mn}_3\text{TeO}_6 + \text{Mn}_3\text{O}_4$ .** The vaporization residues of experiments 22, 26, 46 (series 1), and 28 (series 2c) all retained the three condensed phases ( $\text{MnTeO}_3$ ,  $\text{Mn}_3\text{TeO}_6$ , and  $\text{Mn}_3\text{O}_4$ ) that were initially present. In experiment 23, which was conducted for relatively longer duration with the same starting sample as experiments 22 and 26, the  $\text{MnTeO}_3$  phase had disappeared or depleted to an extent undetectable by X-ray diffraction. The experiment 28 (lone experiment of series 2c) rendered it possible to examine how the vaporization behavior of a sample that represented a three-phase equilibrium of  $\text{MnTeO}_3 + \text{Mn}_3\text{TeO}_6 + \text{vapor}$  would change upon addition of  $\text{Mn}_3\text{O}_4$ . Furthermore, it also confirmed the existence of the four-

phase equilibrium  $\text{Mn}_3\text{TeO}_6 + \text{Mn}_3\text{O}_4 + \text{MnTeO}_3 + \text{vapor}$  observed in experiments 22, 26, and 46.

**Residue  $\text{Mn}_3\text{TeO}_6 + \text{Mn}_3\text{O}_4$ .** Two experiments from series 1 yielded this residue. If in one (experiment 23), it resulted from the disappearance of the  $\text{MnTeO}_3$  phase, in the other (experiment 34), it resulted from the generation of the  $\text{Mn}_3\text{O}_4$  phase afresh upon heating the single phase  $\text{Mn}_3\text{TeO}_6$ . The experiments 10, 11, 12, 14, and 15 of series 2a and the experiments 31, 35, and 36 of series 2b also gave this residue. The added MnO in series 2a or the added Mn in series 2b, as well as the ternary phases on the MnO– $\text{TeO}_2$  binary line, had all disappeared to ultimately yield a two-phase mixture of  $\text{Mn}_3\text{TeO}_6 + \text{Mn}_3\text{O}_4$ . A rather high evolution of tellurium as  $\text{Te}_2(\text{g})$  during the initial stages of heating, disappearance of both MnO and  $\text{MnTeO}_3$ , buildup of  $\text{Mn}_3\text{TeO}_6$ , and formation of  $\text{Mn}_3\text{O}_4$  indicate the following possibilities during series 2a: (1) evolution of  $\text{Te}_2(\text{g})$  occurred due to consumption of excess MnO by  $\text{MnTeO}_3$ , even while the system was being heated to 950 K according to the reaction



(2) the following reaction occurred either simultaneously or sequentially if some MnO were to remain free after completing the task of consuming all  $\text{MnTeO}_3$



**Residue  $\text{MnO} + \text{Mn}_3\text{O}_4$ .** In experiments 24 and 25 of series 2a, however, the MnO phase did remain in the residue (along with  $\text{Mn}_3\text{O}_4$ ), but interestingly, as has been mentioned already, both  $\text{MnTeO}_3$  and  $\text{Mn}_3\text{TeO}_6$  had disappeared. Possibly, the MnO fraction was so high that it had remained even after completion of reactions 1 and 2.

**Residue  $\text{Mn} + \text{MnO} + \text{MnTe}$ .** The experiment 27 of series 2b also yielded the MnO phase but at the cost of all ternary phases that were originally present to coexist with Mn and MnTe. Vaporization behavior of this phase mixture did not permit the system to reach the MnO– $\text{TeO}_2$  binary line because of immeasurably low volatility of this phase mixture.

**Residue  $\text{MnTeO}_3 + \text{Mn}_6\text{Te}_5\text{O}_{16} + \text{Mn}_3\text{O}_4$ .** The experiment 43 of series 1 gave this residue indicating that the three phases originally present could be retained, even after an experimental duration of  $\sim 12$  h at 950 K.

**Vaporization Behavior.** The following inferences may be made from the foregoing discussion of the condensed phases identified in the as-prepared samples and in the vaporization residues: the MnO-rich part of the MnO– $\text{TeO}_2$  system tends not to remain binary at high temperatures; the overall composition of the sample under effusion conditions tends to move away from the MnO– $\text{TeO}_2$  binary line. These aspects, especially the latter, are vaporization chemistry driven and are examined below.

**Four- and Three-Phase Vaporization Equilibria.** In the absence of congruent vaporization (as evidenced by the absence of Mn-bearing vapor species), any univariant vaporization equilibrium (invariant at constant  $T$ ) observed in this system can be one of a four-phase equilibrium type (4PEQ) or a three-phase equilibrium (3PEQ) type. The results of mass spectroscopic experiments in which all three condensed phases (that were initially present) were retained in the residues were ascribed to four-phase equilibria. Thus, the results of experiment 43 corresponded to the four-phase equilibrium  $\text{MnTeO}_3 + \text{Mn}_6\text{Te}_5\text{O}_{16} + \text{Mn}_3\text{O}_4 + \text{vapor}$ , while the results of experiments 22, 26, and 46 corresponded to the four-phase equilibrium  $\text{MnTeO}_3 + \text{Mn}_3\text{TeO}_6 + \text{Mn}_3\text{O}_4 + \text{vapor}$ , denoted as 4PEQ1 and 4PEQ2,

**TABLE 3: Details Pertinent to Vaporization Behavior during Different Equilibria at  $T = 950$  K**

parameter	TeO <sub>2</sub> (s) (congruent effusion)	Mn–Te–O system <sup>a</sup>						
		expt 43 4PEQ1	expts 22 and 23 4PEQ2	expt 23 3PEQ2	expt 16 4PEQ3	expt 16 3PEQ1	expt 18 4PEQ3	expt 18 3PEQ1
		Partial Pressures in Pa						
$p(\text{TeO}_2)$	1.980	0.033	0.021	0.015	0.228	0.052	0.228	0.047
$p(\text{TeO})$	1.190	0.103	0.066	0.051	0.253	0.127	0.253	0.109
$p(\text{Te}_2)$	0.197	0.093	0.062	0.053	0.030	0.047	0.030	0.050
$p(\text{O}_2)^b$	0.420	0.016	0.015	0.012	0.123	0.026	0.123	0.028
Te-to-O Atomic Flow Ratio in the Effusate								
$R_{\text{effusate}}^c$	0.50	1.17	1.06	1.11	0.43	0.74	0.43	0.72
$R_{\text{effusate}}^d$	0.69	1.37	1.70	1.82	0.86	1.48	0.82	1.41

<sup>a</sup> 4PEQ1, MnTeO<sub>3</sub> + Mn<sub>6</sub>Te<sub>3</sub>O<sub>16</sub> + Mn<sub>3</sub>O<sub>4</sub> + vapor; 4PEQ2, Mn<sub>3</sub>O<sub>4</sub> + Mn<sub>3</sub>TeO<sub>6</sub> + MnTeO<sub>3</sub> + vapor; 4PEQ3, Mn<sub>3</sub>TeO<sub>6</sub> + MnTeO<sub>3</sub> + Mn<sub>2</sub>Te<sub>3</sub>O<sub>8</sub> + vapor; 3PEQ1, Mn<sub>3</sub>TeO<sub>6</sub> + MnTeO<sub>3</sub> + vapor; 3PEQ2, Mn<sub>3</sub>O<sub>4</sub> + Mn<sub>3</sub>TeO<sub>6</sub> + vapor. <sup>b</sup>  $p(\text{O}_2)$  was derived employing eq 3 for TeO<sub>2</sub>(s); the same for Mn–Te–O samples were derived from the  $p(\text{TeO}_2)/p(\text{TeO})$  ratios. <sup>c</sup> Relation 3 was employed. <sup>d</sup> Relation 5 was employed.

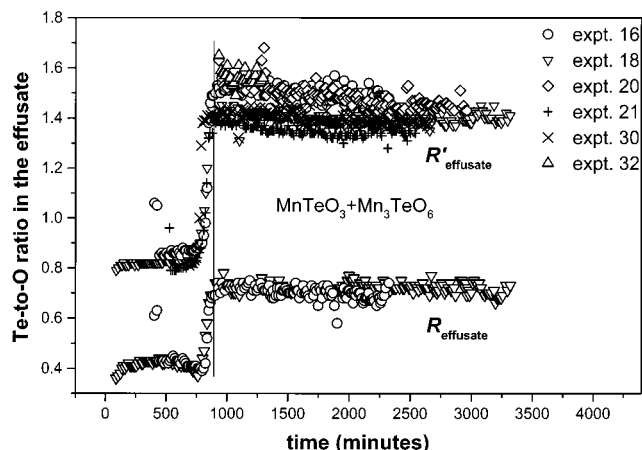
respectively. The initial mass spectrometric results in the experiments 16 and 18 were ascribed to another four-phase equilibrium MnTeO<sub>3</sub> + Mn<sub>3</sub>TeO<sub>6</sub> + Mn<sub>2</sub>Te<sub>3</sub>O<sub>8</sub> + vapor and denoted as 4PEQ3. As mentioned before, many experiments yielded only two condensed phases in the residue: MnTeO<sub>3</sub> + Mn<sub>3</sub>TeO<sub>6</sub> or Mn<sub>3</sub>TeO<sub>6</sub> + Mn<sub>3</sub>O<sub>4</sub>. Existence of three-phase equilibria was assumed in those cases in which the ion intensities remained invariant with time for reasonable duration at the time of termination. For further discussion, the equilibrium MnTeO<sub>3</sub> + Mn<sub>3</sub>TeO<sub>6</sub> + vapor is denoted as 3PEQ1 and the equilibrium Mn<sub>3</sub>TeO<sub>6</sub> + Mn<sub>3</sub>O<sub>4</sub> + vapor as 3PEQ2.

Table 3 compares the results corresponding to different invariant vaporization equilibria (at  $T = 950$  K) including that involving congruent effusion of TeO<sub>2</sub>(s). Because the vapor phase in all cases is composed of only Te- and O-bearing gaseous species, differences in the vaporization behavior can be best understood by rigorously analyzing the Te-to-O atomic flow ratios in the effusates. We will henceforth denote this ratio as  $R_{\text{effusate}}$ , which we calculated by employing the relation

$$R_{\text{effusate}} = \frac{2p(\text{Te}_2)/\sqrt{M(\text{Te}_2)} + p(\text{TeO})/\sqrt{M(\text{TeO})} + p(\text{TeO}_2)/\sqrt{M(\text{TeO}_2)}}{p(\text{TeO})/\sqrt{M(\text{TeO})} + 2p(\text{TeO}_2)/\sqrt{M(\text{TeO}_2)} + 2p(\text{O}_2)/\sqrt{M(\text{O}_2)}} \quad (3)$$

where  $p(i)$  and  $M(i)$  refer to partial pressure and mean molar mass of the gaseous species  $i$ , respectively. The required  $p(i)$ s (except where  $i = \text{O}_2$ ) were those computed from the  $p(i) - T$  relations given by Lakshmi Narasimhan<sup>20</sup> for TeO<sub>2</sub>(s) and the four-phase equilibria. The  $p(i)$ s for the three-phase equilibria 3PEQ1 and 3PEQ2 were computed as  $I(i^+)/k(i)$  where  $k(i)$  is the pressure calibration constant. The  $k(i)$ s for 3PEQ1 were obtained in situ from  $p(i)/I(i^+)$  during the 4PEQ3 of experiments 16 and 18. In the same way, the  $k(i)$ s for the 3PEQ2 were obtained in situ from  $p(i)/I(i^+)$  during the 4PEQ2 of experiment 23. Because the  $I(\text{O}_2^+)$  measured by us was not precise enough to deduce meaningful  $p(\text{O}_2)$ , we estimated the  $p(\text{O}_2)$ s in the following way: the  $p(\text{O}_2)$  over congruently effusing TeO<sub>2</sub>(s) was first computed by inputting in eq 3 the  $p(i)$ s of other species and a value of  $R_{\text{effusate}} = 0.5$ ; subsequently, the  $p(\text{O}_2)$ s corresponding to the different equilibria in the Mn–Te–O system were calculated from the  $p(\text{TeO})/p(\text{TeO}_2)$  ratios over the Mn–Te–O system and over TeO<sub>2</sub>(s).

Table 3 shows that the  $R_{\text{effusate}}$  values for all of the vaporization equilibria observed by us in the Mn–Te–O system (except that for 4PEQ3) are higher than that for the congruent effusion of TeO<sub>2</sub>(s). This supports the inference made above with regard to the continuous movement of condensed-phase composition away from the MnO–TeO<sub>2</sub> binary line.

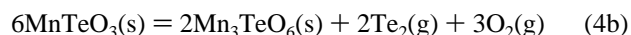
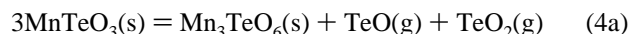


**Figure 6.** Te-to-O atomic flow ratios in the effusates (true,  $R_{\text{effusate}}$ , and apparent,  $R'_{\text{effusate}}$ ) during different vaporization experiments, which yielded in residues the two condensed phases: MnTeO<sub>3</sub> + Mn<sub>3</sub>TeO<sub>6</sub>. For clarity, an incremental addition  $\Delta t$  was given to the starting time of all experiments except 18. Hence,  $t = t_{\text{shown}} - \Delta t$ , and  $\Delta t = 0, 330, 831, 423, 600$ , and  $829$  min for experiments 18, 16, 20, 21, 30, and 32, respectively.

The variation of  $R_{\text{effusate}}$  as a function of time for experiments 16 and 18 is shown in Figure 6. The values initially were  $\sim 0.43$ , then increased steeply to  $\sim 0.73$ , and remained invariant with time until the termination of these experiments. The partial pressures and the  $R_{\text{effusate}}$  values corresponding to the univariant vaporization equilibria 4PEQ3 and 3PEQ1 that occurred in these experiments are listed in Table 3. The value of  $R_{\text{effusate}} = 0.43$  during the 4PEQ3 is very close to that for the congruent effusion TeO<sub>2</sub>(s), clearly indicating that during the 4PEQ3 the tendency to move away from the MnO–TeO<sub>2</sub> binary line was absent.

The variation of  $R_{\text{effusate}}$  values as a function of time for the experiment 23 is shown in Figure 7. The values of  $R_{\text{effusate}}$  during the final period (3PEQ2) were only very slightly higher than those during the initial part of the experiment (4PEQ2). The  $R_{\text{effusate}}$  values of both 4PEQ2 and 3PEQ2 (see Table 3) are 2 times higher than that for the congruent effusion of TeO<sub>2</sub>(s).

The restriction concerning the invariant 3PEQ1 emerges by examining the following simultaneous reactions:



For the equilibrium 4 to remain invariant (at constant  $T$ ), the  $R_{\text{effusate}}$  value must be  $2/3$ . We obtained values of  $R_{\text{effusate}} = 0.74$  and  $0.72$  (experiments 16 and 18, respectively; see Table 3), in accord with the restriction requirement. A number of other



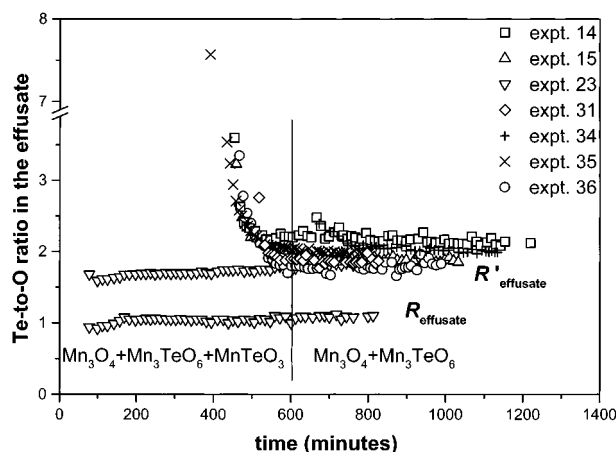


**Figure 7.** Te-to-O atomic flow ratios in the effusates (true,  $R_{\text{effusate}}$ , and apparent,  $R'_{\text{effusate}}$ ) during different vaporization experiments, which yielded in residues the two condensed phases:  $\text{Mn}_3\text{TeO}_6 + \text{Mn}_3\text{O}_4$ .  $t = t_{\text{shown}} - \Delta t$ , and  $\Delta t = 0, 382, 371, 150, 572, 268$ , and  $281$  min for experiments 23, 14, 15, 31, 34, 35, and 36, respectively.

experiments yielded  $\text{MnTeO}_3 + \text{Mn}_3\text{TeO}_6$  as vaporization residues and thus permit their end-results being classified under 3PEQ1. A direct verification of the restriction ( $R_{\text{effusate}} = 2/3$ ) in these cases was hampered by the absence of pressure calibration constants, in situ or external. Therefore, we resorted to calculation of what we would term as  $R'_{\text{effusate}}$  (“apparent” Te-to-O ratios). Rearrangement of relation 3 after setting  $p(\text{O}_2) = 0$  and substituting partial pressures of other species with ion intensities yields

$$R'_{\text{effusate}} = \frac{1 + XR_x\sqrt{M(\text{TeO}_2)/M(\text{TeO})} + 2YR_y\sqrt{M(\text{TeO}_2)/M(\text{Te}_2)}}{2 + XR_x\sqrt{M(\text{TeO}_2)/M(\text{TeO})}} \quad (5)$$

where  $X = I(\text{TeO}^+)/I(\text{TeO}_2^+)$ ,  $Y = I(\text{Te}_2^+)/I(\text{TeO}_2^+)$ ,  $R_x$  is the factor that converts  $X$  to  $p(\text{TeO})/p(\text{TeO}_2)$ , and  $R_y$  is the factor that converts  $Y$  to  $p(\text{Te}_2)/p(\text{TeO}_2)$ . The factors  $R_x$  and  $R_y$  were obtained by converting the ion intensities measured at 37.3 eV to those at 13.0 eV and by using ionization cross sections ( $\sigma$ ) at 13.0 eV, and relative detector responses ( $\gamma$ ). The ionization cross sections for  $\sigma(\text{Te}_a\text{O}_b)$  were estimated by using the empirical relation  $\sigma(\text{Te}_a\text{O}_b) = 0.75[a\sigma(\text{Te}) + b\sigma(\text{O})]$  and the values of  $\sigma(\text{Te})$  and  $\sigma(\text{O})$  from Mann’s compilation.<sup>21</sup> The relative detector response for each ion was deduced by measuring the ion intensities on at least one occasion with both secondary electron multiplier and Faraday cup. The variation of  $R'_{\text{effusate}}$  values as a function of time for the experiments 16, 18, 20, 21, 30, and 32 are shown in Figure 6. The  $R'_{\text{effusate}}$  values during the final phase of all these experiments appear consistent within  $1.5 \pm 0.1$ . In this exercise, the experiments 16 and 18 served as internal references ( $R_{\text{effusate}} = 0.73 \pm 0.1$ ) and provided evidence for the existence of 3PEQ1 in other four experiments, too. The results from experiments 7, 8, and 9 were excluded in this exercise, although they also gave stable ion intensities, because of some doubts about the reliability of the  $R_x$  and  $R_y$  values for these experiments arising from inconsistent ion-source performance during that period.

An additional evidence that the seemingly endless univariant vaporization equilibrium, which we observed in experiments 16, 18, 21, and 30 (see Figures 1–4), was indeed a 3PEQ and not a 4PEQ was obtained from the experiment 28 of series 2c. The sample for this experiment, as mentioned already, was prepared by adding a little  $\text{Mn}_3\text{O}_4$  phase to the residues from

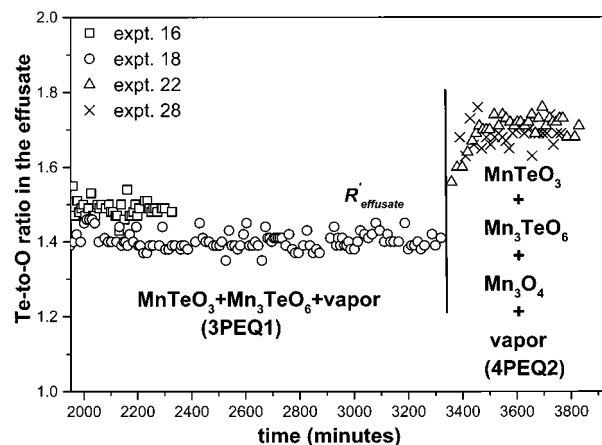
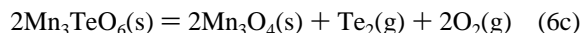
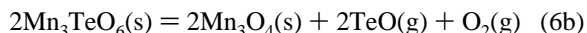
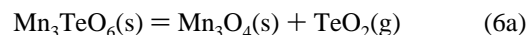


**Figure 8.** Apparent Te-to-O atomic flow ratios during the three-phase equilibrium 3PEQ1 ( $\text{MnTeO}_3 + \text{Mn}_3\text{TeO}_6 + \text{vapor}$ ) and during the four-phase equilibrium 4PEQ2 ( $\text{MnTeO}_3 + \text{Mn}_3\text{TeO}_6 + \text{Mn}_3\text{O}_4 + \text{vapor}$ ).  $t = t_{\text{shown}} - \Delta t$ , and  $\Delta t = 0, 330, 3287$ , and  $3287$  min for experiments 18, 16, 28, and 22, respectively.

experiments 16 and 18 (biphasic  $\text{MnTeO}_3 + \text{Mn}_3\text{TeO}_6$ ). Figure 8 reveals that the  $R'_{\text{effusate}}$  values for this sample were no longer the same as those that existed in experiments 16 and 18 but instead rose to values in accord with those for the 4PEQ2 obtained in experiment 22 (see also Table 3).

The restriction concerning the invariant 3PEQ2 emerges by examining the following simultaneous reactions:



For the equilibrium 6 to remain invariant (at constant  $T$ ), the  $R_{\text{effusate}}$  value must be  $1/2$ . The  $R_{\text{effusate}}$  obtained in experiment 23, as shown in Figure 7 and Table 3, reveals that it was rather high ( $\sim 1.1$ ), discordant with the restriction requirement. A plot of how  $R'_{\text{effusate}}$  varied as a function of time in the experiment 23, as well as in many other experiments (14, 15, 31, 34, 35, and 36) is shown in Figure 7. The  $R'_{\text{effusate}}$  values during the final phase of all of these experiments were consistent within  $2.0 \pm 0.2$ . Thus, unlike in the case of the 3PEQ1, a convincing evidence for the existence of the 3PEQ2 eluded us. For it to be classified as a 4PEQ, the “missing third condensed phase” has to be identified. Whatever be the latter, the  $R_{\text{effusate}}$  for that unknown four-phase equilibrium is very close to that of the 4PEQ2. Interestingly, the adjacent 4PEQ1 also has a  $R_{\text{effusate}}$  value very nearly the same as 4PEQ2 (see Table 3). Only through a prolonged vaporization may we be able to generate the third condensed phase sufficiently for its detection by X-ray diffraction. If this phase were to lie above the  $\text{Mn}_3\text{O}_4$ – $\text{TeO}_2$  line, as the value of  $R_{\text{effusate}} \approx 1.1$  will lead us to believe, it could be a ternary phase (e.g.,  $\text{Mn}_2\text{TeO}_6$ ).

**Anomalous Vaporization.** We now discuss some common and interesting features revealed in Figures 1–4. The variation of ion intensities (in arbitrary units) with time, as obtained in experiments 16, 18, 21, and 30, respectively, are shown in these figures. In the case of  $I(\text{O}_2^+)$ , the values are not those measured but actually  $[p(\text{TeO}_2)/p(\text{TeO})]^2 = (XR_x)^{-2}$ , where  $X$  and  $R_x$  denote the same quantities as those described in eq 5.

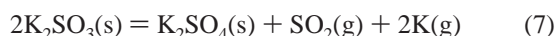
In experiments 16 (Figure 1) and 18 (Figure 2), there initially was some semblance of stability for  $\sim 2$  h in ion intensities (4PEQ3;  $\text{Mn}_2\text{Te}_3\text{O}_8 + \text{MnTeO}_3 + \text{Mn}_3\text{TeO}_6 + \text{v}$ ), before they started decreasing monotonically. In experiments 21 (Figure 3)

and 30 (Figure 4), it was a continuous decrease immediately upon attainment of 950 K. The relative amount of  $\text{Mn}_2\text{Te}_3\text{O}_8$  in the aliquots of samples used in experiments 21 and 30 was perhaps so small that the 4PEQ3 never existed long enough to yield stable intensities at 950 K. The monotonic decreases in the ion intensities were attributed to the system becoming bivariant after the disappearance of  $\text{Mn}_2\text{Te}_3\text{O}_8$ . All intensities reached invariancy around the minimum values, except that of  $\text{Te}_2^+$ . The  $I(\text{Te}_2^+)$ , after reaching a minimum, increased rapidly to reach a value that was 3 to 4 times higher. Furthermore, as shown for experiment 18 in Figure 2, the ion intensities of  $\text{TeO}_2^+$  and  $\text{TeO}^+$  and during the eventual 3PEQ1 were lower (by a factor of 4.8 and 2.3, respectively) than those during 4PEQ3, whereas that of  $\text{Te}_2^+$  was higher by a factor of 1.6.

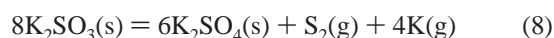
We believe that the above observations must be related to a sequence of events concerning the transition from 4PEQ3 to 3PEQ1. This transition involves the disappearance of the condensed phase  $\text{Mn}_2\text{Te}_3\text{O}_8$  and an increase in the atomic flow ratios of tellurium and oxygen from that due to the initial univariant 4PEQ3 ( $\sim 0.43$ ) to that due to the final 3PEQ1 ( $\sim 0.73$ ). For effecting such a change in the values of  $R_{\text{effusate}}$ , and perhaps also changes in the stoichiometries of  $\text{MnTeO}_3$  or  $\text{Mn}_3\text{TeO}_6$  or both (different from those during the initial 4PEQ3 and appropriate for the final 3PEQ1), the partial pressures of the various Te- and O-bearing species must vary suitably. The turn around in the  $I(\text{Te}_2^+)$  in the intervening bivariant period was then a consequence of such a necessity.

$Te(IV) = Te(VI)$ . It is clear from above discussion that the 4PEQ3 does not lead to the 4PEQ2 but instead to the 3PEQ1, which separates them and will remain univariant. This aspect together with many observations made in the present study such as the presence of  $\text{Mn}_3\text{TeO}_6$  in most of the samples and vaporization residues and high amounts of  $\text{Te}_2(\text{g})$  evolution in series 2a and 2b experiments lend support to the observation and inference made by Trömel and Schmid<sup>15</sup> that when  $x(\text{MnO}) \geq 0.5$ , disproportionation of the  $(\text{MnO})_x(\text{TeO}_2)_{1-x}$  phase (tellurium as  $\text{Te(IV)}$ ) to elemental tellurium and  $\text{Mn}_3\text{TeO}_6$  (tellurium as  $\text{Te(VI)}$ ) occurred. The relatively greater stability of  $\text{Te(VI)}$  at high temperatures perhaps made the vaporization chemistry of the Mn–Te–O system complex and interesting.

Evidence for similar complex vaporization associated with a  $(IV) = (VI)$  equilibrium was previously obtained by Edwards<sup>22</sup> in the case of the fellow chalcogen, sulfur. Upon investigation of the system  $\text{K}_2\text{SO}_3$  at  $T = 1100\text{--}1200$  K, Edwards found that the gaseous species  $\text{SO}_2$ ,  $\text{S}_2$ , and K were produced because of the following reactions:



and



Although Edwards could not obtain equilibrium (and thus the relative proportions of the gaseous species), the study served to indicate the great stability at high temperatures of  $\text{S(VI)}$ , that is,  $\text{K}_2\text{SO}_4(\text{s})$ . Our ongoing study of  $x\text{NiO} + (1-x)\text{TeO}_2$  (with  $x > 0.5$ ) has however not shown the kind of disproportionation shown by the Mn–Te–O system, although the phase  $\text{Ni}_3\text{TeO}_6$  could be prepared in a way similar to  $\text{Mn}_3\text{TeO}_6$ . It might be that, in addition to the stability of  $\text{Te(VI)}$ , the chemical property of the metal oxide would also be a factor that would decide disproportionation. Trömel and Schmid<sup>14</sup> hypothesized that the  $\text{Te(IV)}$  to  $\text{Te(VI)}$  disproportionation would occur when the lattice energy of the bivalent basic oxide is less than  $\sim 4000$  kJ  $\text{mol}^{-1}$ .

## Conclusions

The vaporization study presented in this paper represents the first to have been conducted in the Mn–Te–O system. We chose to present only the aspects concerning the complexities associated with preparation of and effusion measurements on samples of  $x\text{MnO} + (1-x)\text{TeO}_2$  with  $x \geq 0.5$ . That the phase  $\text{Mn}_6\text{Te}_5\text{O}_{16}$  could remain stable at  $T = 950$  K under effusion conditions was shown by the evidence obtained for the 4PEQ1 (experiment 43). However, we failed in all of our attempts to obtain this phase coexisting with  $\text{MnO}(\text{s})$ , due mostly to the vaporization behavior that involved preferential loss of tellurium relative to oxygen. We succeeded when we undertook the preparations starting with  $\text{Mn} + \text{MnO} + \text{TeO}_2$  or  $\text{Mn} + \text{MnO} + \text{Mn}_3\text{TeO}_6$  mixtures. More details about sample preparations, determination of the Mn–Te–O phase diagram in and around the MnO– $\text{TeO}_2$  binary line, and the thermodynamic properties of the pertinent ternary phases are given in a paper<sup>23</sup> under preparation.

**Acknowledgment.** We thank Dr. G. Periaswami, Head, Materials Chemistry Division, for his encouragement during this study. We also thank the X-ray group for their great help in the characterization of samples and the electronics group for the maintenance of the mass spectrometer.

## References and Notes

- (1) Adamson, M. G.; Aitken, E. A.; Lindemer, T. B. *J. Nucl. Mater.* **1985**, *130*, 375.
- (2) Viswanathan, R. Ph.D. Thesis, University of Madras, Madras, India, **1991**.
- (3) Lakshmi Narasimhan, T. S.; Balasubramanian, R.; Nalini, S.; Sai Baba, M. *J. Nucl. Mater.* **1997**, *247*, 28.
- (4) Saha, B.; Viswanathan, R.; Sai Baba, M.; Darwin Albert Raj, D.; Balasubramanian, R.; Karunasagar, D.; Mathews, C. K. *J. Nucl. Mater.* **1985**, *130*, 316.
- (5) Sai Baba, M.; Viswanathan, R.; Balasubramanian, R.; Darwin Albert Raj, D.; Saha, B.; Mathews, C. K. *J. Chem. Thermodyn.* **1988**, *20*, 1157.
- (6) Viswanathan, R.; Sai Baba, M.; Darwin Albert Raj, D.; Balasubramanian, R.; Saha, B.; Mathews, C. K. *J. Nucl. Mater.* **1987**, *149*, 302.
- (7) Viswanathan, R.; Sai Baba, M.; Darwin Albert Raj, D.; Balasubramanian, R.; Saha, B.; Mathews, C. K. *J. Nucl. Mater.* **1989**, *167*, 94.
- (8) Viswanathan, R.; Sai Baba, M.; Lakshmi Narasimhan, T. S.; Balasubramanian, R.; Darwin Albert Raj, D.; Mathews, C. K. *J. Alloys Compd.* **1994**, *206*, 201.
- (9) Viswanathan, R.; Balasubramanian, R.; Mathews, C. K. *J. Chem. Thermodyn.* **1989**, *21*, 1183.
- (10) Viswanathan, R.; Darwin Albert Raj, D.; Lakshmi Narasimhan, T. S.; Balasubramanian, R.; Mathews, C. K. *J. Chem. Thermodyn.* **1993**, *25*, 533.
- (11) Sai Baba, M.; Lakshmi Narasimhan, T. S.; Balasubramanian, R.; Mathews, C. K. *J. Nucl. Mater.* **1993**, *201*, 147.
- (12) Lakshmi Narasimhan, T. S.; Viswanathan, R.; Balasubramanian, R. *J. Phys. Chem. B* **1998**, *102*, 10586.
- (13) Lakshmi Narasimhan, T. S.; Sai Baba, M.; Balasubramanian, R.; Nalini, S.; Viswanathan, R. *J. Chem. Thermodyn.* **2002**, *34*, 103.
- (14) Trömel, V. M.; Schmid, D. Z. *Anorg. Allg. Chem.* **1972**, *387*, 230.
- (15) Trömel, V. M.; Scheller, Th. Z. *Anorg. Allg. Chem.* **1976**, *427*, 229.
- (16) Bayer, G. Z. *Kristallogr.* **1967**, *124*, 131.
- (17) Ivanova, Y. Y. *Mater. Chem.* **1982**, *7*, 449.
- (18) Gospodinov, G. G.; Mihov, D. I. *J. Chem. Thermodyn.* **1993**, *25*, 1249.
- (19) Lesar, A.; Popovic, A.; Marsel, J. J. *Less-Common Met.* **1988**, *143*, 151.
- (20) Lakshmi Narasimhan, T. S. Ph.D. Thesis, University of Madras, Madras, India, 2000.
- (21) Mann, J. B. Recent Developments in Mass Spectrometry. In *Proceedings of the International Conference on Mass Spectrometry*; Ogata, K., Hayakawa, T., Eds.; University of Tokyo Press: Tokyo, Japan, 1970; p 814.
- (22) Edwards, J. G. Personal communication.
- (23) Lakshmi Narasimhan, T. S.; Sai Baba, M.; Viswanathan, R., manuscript in preparation.